

Experiment and Modeling of Conversion of Substrate-Waveguided Modes to Surface-Emitted Light by Substrate Patterning

Min-Hao M. Lu, Conor F. Madigan, and J. C. Sturm

Center for Photonic and Optoelectronic Materials, Department of Electrical Engineering, Princeton University, Princeton, NJ 08544, U.S.A.

ABSTRACT

To predict the optical power that could be harvested from light emission that is waveguided in the substrate of organic light emitting devices (OLEDs), a quantitative quantum mechanical model of the light emitted into the waveguided modes has been developed. The model was used to compute the exact distribution of energy in external, substrate and ITO/organic modes as a function of the distance of the emission zone from the cathode. The results are compared to the classical ray optics model and to experiments in two-layer OLED devices. Classical ray optics is found to substantially over-predict the light in waveguided modes.

INTRODUCTION

OLEDs have received enormous interest because of their promise for cheaper and more efficient flat panel displays. A large amount of light is trapped in the substrate due to total internal reflection; therefore, substrate patterning can be used to increase external coupling efficiency [1-3]. The exact distribution of optical energy in all of the waveguide modes has not been calculated previously, except for by classical ray optics. The goal of this paper is to develop such a quantitatively accurate model of such waveguided light and verify it with experiments.

The radiative modes can be classified into external, substrate and ITO/organic modes (Figure 1a). External modes are those with angle to the surface normal in the organic layer less than the critical angle between air and Alq₃, $\theta_{c1} = \sin^{-1} n_{\text{air}}/n_{\text{alq}}$; substrate modes are those with angle between θ_{c1} and the critical angle between glass and Alq₃, $\theta_{c2} = \sin^{-1} n_{\text{glass}}/n_{\text{alq}}$; and

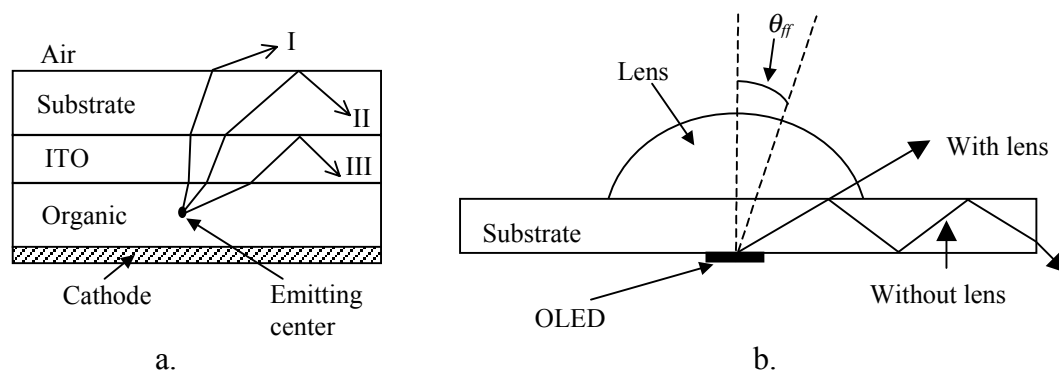


Figure 1. a. Three radiative modes in OLEDs: I. External modes, II. Substrate modes, and III. ITO/organic modes. B. Attaching a lens to the back side of OLED converts some light in substrate modes into external modes [3].

ITO/organic modes are those with angle greater than θ_{c2} . Substrate modes are emitted through the edges of the substrate, whereas the ITO/organic modes are heavily attenuated, and does not emit through the edge [5]. According to classical ray optics the amount of energy emitted into the external, substrate and ITO/organic modes are 18.9%, 34.2% and 46.9%, respectively, for refractive indices of $n_{\text{alq}} = 1.71$, $n_{\text{glass}} = 1.51$, and $n_{\text{air}} = 1$.

By laminating lens arrays on the backside of the OLEDs, some of the light waveguided in the substrate is allowed to emit externally (Figure 1b). For example, Figure 3a shows the far-field emission intensity with and without a lens attached to an OLED made with a single layer poly-(N-vinylcarbazole) (PVK) blend [3]. In one case, the OLED was 2.3 mm below the center of curvature of the lens, and there is a strong focusing effect. Intensity in the normal direction was increased by a factor of 9.5. In another case, the OLED was near the center of curvature of the lens and the total external emission was increased by a factor of 2.0. To understand how much light can be harvested by such techniques, ray optics is not adequate due to microcavity and other quantum mechanical effects in OLED structure. Therefore, in this paper we develop the full theory of light emission into waveguided modes and compare it with experiments.

THEORY

Field quantization in one-sided leaky microcavities was developed in an early paper [4]. Microcavity effects in OLEDs were first investigated by Bulovic et al. [5], whose treatment we follow closely.

The exciton recombination is modeled as a radiating dipole. The total energy transfer rate from the dipole is:

$$W_{\text{Tot}} = W_{\text{ext}} + W_{\text{sub}} + W_{\text{ITO-org}} + W_{\text{DM-SP}} + W_{\text{NR}}$$

where W_{ext} , W_{sub} and $W_{\text{ITO-org}}$ are the transfer rates into the external, substrate-wave guided and ITO/organic modes. $W_{\text{DM-SP}}$ denotes the dipole-metal energy transfer, and W_{NR} the non-radiative energy transfer due to system-crossing. The external efficiency can be found as η_{ext} :

$$\eta_{\text{ext}} = (W_{\text{ext}}/W_0)(W_0/W_{\text{Tot}})$$

where W_0 is the rate in free space. To compute W_{ext}/W_0 due to the microcavity effect we first compute the transition rates which are given by Fermi's golden rule:

$$f = \frac{2\pi}{h} \sum_n |\langle m | \boldsymbol{\mu} \cdot \mathbf{E}(\mathbf{k}, z) | n \rangle|^2 \delta(E_n - E_m - h\nu)$$

where $\boldsymbol{\mu}$ is the dipole moment and $\mathbf{E}(\mathbf{k}, z)$ is the electrical field for mode \mathbf{k} at location of the dipole. E_m and E_n are the energies of the initial and final exciton states. $h\nu$ is the energy of the photon emitted. The total transition rate is obtained by summing over all \mathbf{k} , and ν . The electric field is determined by the microcavity structure:

$$\mathbf{E}_{\mathbf{k}}^{TE} = \mathbf{A}(\mathbf{k}) \sin^2(k_{oz}l) \mathbf{x}$$

$$\mathbf{E}_{\mathbf{k}}^{TM} = \mathbf{B}(\mathbf{k}) \cos^2 \theta_o \sin^2(k_{oz}l) \mathbf{y} + \mathbf{C}(\mathbf{k}) \sin^2 \theta_o \cos^2(k_{oz}l) \mathbf{z}$$

where $\mathbf{A}(\mathbf{k})$, $\mathbf{B}(\mathbf{k})$ and $\mathbf{C}(\mathbf{k})$ are functions of material constants and \mathbf{k} . k_{oz} is the z component of the wave vector in the emitting layer. l is the distance of the emitting center to the cathode. And θ_o is the angle of the mode in the emitting layer. For spontaneous emission, the electrical fields are normalized such that the energy in each mode is equal to that of a single photon. In our two-layer OLEDs, we assume the excitons are created at the PVK/Alq₃ interface, and diffuse into Alq₃ with a characteristic length of 20 nm [5].

The ratio W_o/W_{Tot} is calculated by considering the intrinsic PL efficiency and the quenching effect of a metal surface next to the dipole, which has been solved classically via the Green's function method [6,7]. It has been computed for a 250 nm Alq₃/α-NPD/ITO waveguide, which we will use as an estimate for our OLEDs [5]. We note that the cathode quenching effect diminishes rapidly as the dipole moves away from the metal surface, and virtually disappears once the dipole is 60 – 80 nm away.

EXPERIMENTAL DETAILS

OLEDs were fabricated on O₂ plasma treated, indium tin oxide (ITO, 180 nm, $n_{ITO} = 1.8$) soda lime glass ($n_{glass} = 1.51$) purchased from Applied Films Co. [8]. The hole transporting layer was 80 nm PVK ($n_{PVK} = 1.67$) deposited by spin-coating. The electron transporting and emitting layer was aluminum *tris*(8-hydroxyquinoline) (Alq₃, $n_{alq} = 1.71$) deposited by vacuum sublimation. Its thickness was varied from 20 to 80 nm. The cathode was 50 nm of Mg:Ag (10:1) followed by a thick Ag cap, deposited by evaporation through a shadow mask with 1.7 mm diameter holes. The energy band diagram of these devices is shown in Figure 2. The two-layer OLED structure was used to precisely control the location of the exciton creation and emission. This is because the model results depend critically on the cathode-exciton distance, and this distance is not well known in single-layer devices.

In some cases, a plano-convex lens of radius 3.4 mm was attached to the backside of the OLEDs by index matching gel. The resulting effective substrate thickness is 1.1 mm. The far-field intensity was measured as a function of polarization both with and without the lens. Emission out of the edge of the glass was measured by placing the substrate through the thin slit of a black diaphragm and directly against a photo detector. The substrates were diced, thus the

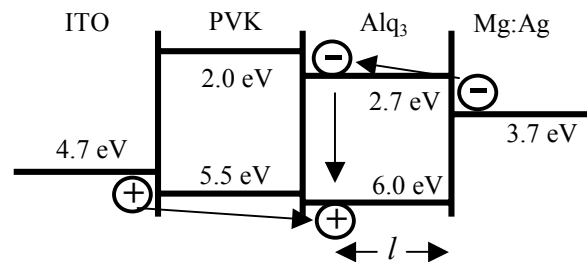


Figure 2. Energy band diagram of the OLEDs. The distance between the recombining exciton and the cathode, l , is controlled by the thickness of the Alq₃ layer. Excitons are assumed to be created at the Alq₃/PVK interface.

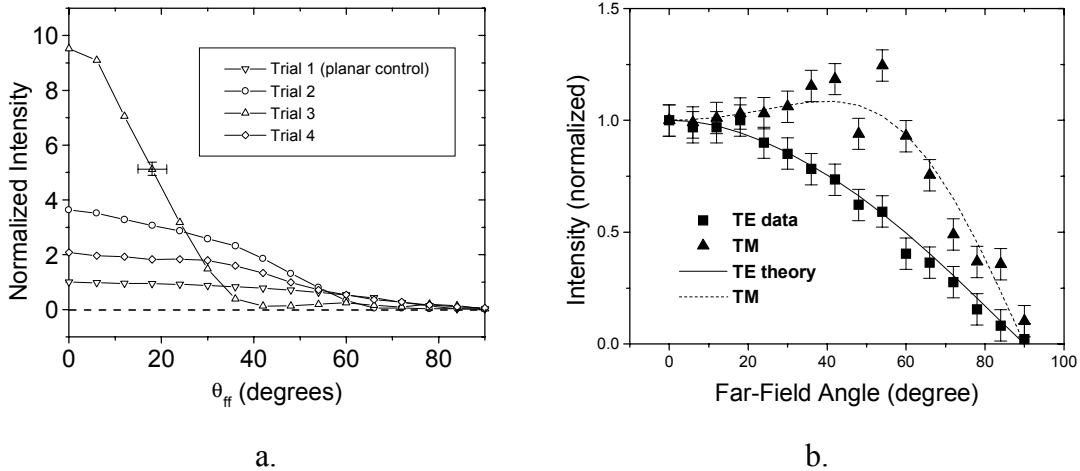


Figure 3. a. Far-field intensity patterns of single-layer OLEDs with planar substrate and with lenses of various geometry. b. Modeling and experimental data of far-field intensity pattern of a planar two-layer OLED with a 20 nm Alq₃ layer. Solid square and upper triangle: measured TE and TM intensity. Solid and dashed lines: theory.

edges are flat but not optically clear, acting as a diffusive scatterer. With this method the change in the optical energy in the substrate modes can be directly measured.

RESULTS AND DISCUSSION

The polarization resolved far-field intensity profile for a device with a 20 nm Alq₃ layer with a planar substrate (no lens) is plotted along with the theoretical prediction (Figure 3b). The fit between theory and data is excellent, reproducing the peak in the TM intensity profile which is a non-classical phenomenon due to the fact that TM radiation is enhanced for an exciton close to the cathode – a microcavity effect.

The QM microcavity model can be used to compute light emission into various modes. The external modes are a continuum. So are the substrate modes since the substrate is much thicker than the ITO/organic layer and the wavelengths in question. ITO/organic modes are discrete. For most of the wavelengths, there is only one TE and one TM mode in the ITO/organic waveguide. However, due to spatial confinement and the normalization condition, the energy in them is still significant. The energy in external and substrate modes is found by integrating over wave vector \mathbf{k} for each mode (a 3-D integral in \mathbf{k} -space), the exciton profile, and the Alq₃ emission spectrum. The energy in ITO/organic modes is computed in the same fashion, except that the 3-D integral is replaced by a discrete sum and a 2-D integral in \mathbf{k} -space. The calculated energy distribution is plotted in Figure 4. As Alq₃ thickness is increased from 20 to 80 nm, total light emission, external light emission, and the percentage of external light emission all increases. For devices with a thick Alq₃ layer (60-80 nm), approximately 35% of the total light generated is emitted externally. This is substantially larger than the 18.9% external emission given by classical ray optics. The highest external quantum efficiency, η_{ext} , measured in an 80-nm-Alq₃ planar device was 0.9%, from which we infer that approximately 10% of injected electrons produce singlet excitons [5].

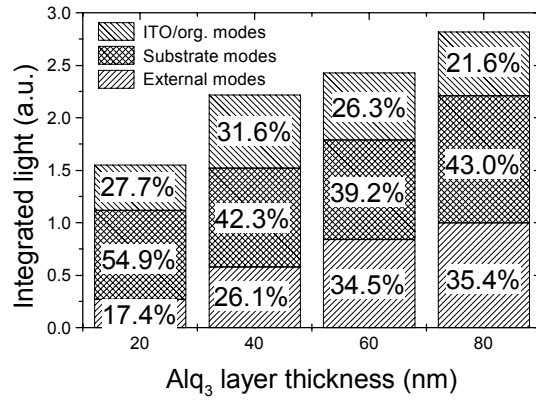


Figure 4. Distribution of energy into external, substrate and ITO/organic modes as a function of Alq₃ thickness. The energy in the external modes is normalized according to measurement. The percentages are calculated from the model. The energy in the substrate and ITO/organic modes is computed from the ratio of the percentages.

We now look at simultaneous measurements of external and edge emission before and after a lens is attached. Since light in ITO/organic modes suffer from high propagation loss, all the light entering the edge detector are from the substrate modes [5]. We define r_1 and r_2 as the ratio of external and edge emissions before and after attaching the lens. The lens does not alter the spatial energy distribution of external modes which is predominantly in air. Furthermore, the substrate is much thicker than the wavelengths in question, any change at the backside of the substrate should not affect the ITO/organic microcavity; therefore, the total light emission is assumed to be the same before and after attaching the lens. Then the ratio of energy emitted into the external and substrate modes (which is equal to η_{ext}/η_{sub}) can be calculated directly from r_1 and r_2 . For a sample with an 80 nm Alq₃ layer, r_1 and r_2 were found to be 1.75 ± 0.12 and 0.30 ± 0.05 respectively, which implies a η_{ext}/η_{sub} of $93 \pm 20\%$. In comparison, classical ray optics gives $\eta_{ext}/\eta_{sub} = 55\%$, and our model gives $\eta_{ext}/\eta_{sub} = 83\%$. The model clearly gives much better agreement with experimental data.

For display systems engineering, it is important to know how much light can be harvested by substrate patterning. Due to the finite size of the lenses, we examine light emission only in a 120° cone, because modes with larger angles run into edge of the lens. Total integrated light emission in this cone before and after attaching the lens is measured experimentally and computed by the model (Figure 5). For devices with thick Alq₃ layer (60-80 nm), the agreement between data and modeling result is well within the experimental error. Both give an increase by a factor of 2.10. The model over-predicts the amount of increase at thinner Alq₃ thickness. We believe the discrepancy originates from the estimate of cathode quenching effect, which is critical for excitons located near the cathode. On the other hand, classical ray optics predicts an increase by a factor of 3.2 in all devices. Again, our model fits the data better, especially at higher Alq₃ layer thickness.

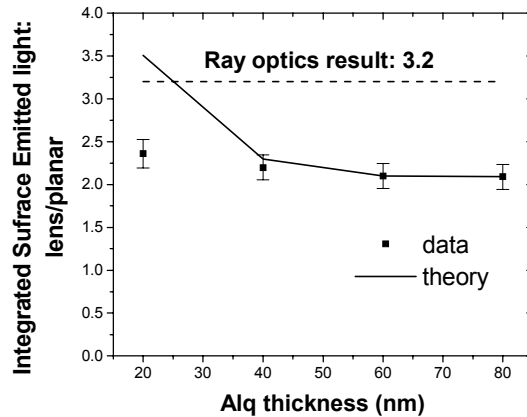


Figure 5. Modeling and experimental data for the improvement factor in total integrated light in the forward 120° cone as a result of attaching a lens as a function of Alq₃ layer thickness. Ray optics predicts an improvement of 3.2X.

CONCLUSIONS

We developed a quantum mechanical microcavity model for OLEDs to compute light emission into the external, substrate and ITO/organic modes. The validity of the model is verified by good fits to far-field intensity and edge emission data. The model also accurately predicts the increase of externally emitted light as a result of attaching a lens to an OLED with thick Alq₃ layers (60-80 nm). Ray optics was found to over-predict both the fraction of waveguided light and the increase due to attaching a lens.

ACKNOWLEDGEMENTS

M.-H. Lu would like to thank V. Bulovic for helpful discussions. This work is supported by DARPA and NSF.

REFERENCES

1. G. Gu, D. Z. Garbuzov, P. E. Burrows, S. Venkatesh, and S. R. Forrest, *Opt. Lett.*, **22**, 396 (1997).
2. T. Yamasaki, K. Sumioka, and T. Tsutsui, *App. Phys. Lett.*, **76**, 1243, (2000).
3. C. Madigan, M.-H. Lu, J. C. Sturm, *App. Phys. Lett.*, **76**, 1650 (2000).
4. K. Ujihara, *Phys. Rev. A*, **12**, 148 (1975).
5. V. Bulovic, V. B. Khalfin, G. Gu, and P. E. Burrows, D. Z. Garbuzov, and S. R. Forrest, *Phys. Rev. B*, **58**, 3730 (1998).
6. R. R. Chance, A. Prock, and R. Sibley, *Adv. in Chem. Phys.*, **37**, 1 (1978).
7. D. Z. Garbuzov, V. Bulovic, P. E. Burrows, and S. R. Forrest, *Chem. Phys. Lett.*, **249**, 433 (1996).
8. C.-C. Wu, J. C. Sturm, R. A. Register, J. Tian, E. P. Dana, and M. E. Thomson, *IEEE Tran. Elec. Dev.*, **44**, 1269 (1997).